

## 2.4 Search for New Phenomena

### 2.4.1 Introduction

We know that the Standard Model is incomplete—it has a non-physical high-energy behavior, and also lacks the deep explanatory power that we seek in a fundamental theory of space-time, forces, and particles. There is currently a great deal of theoretical activity focussed on new physics that would solve the problems with the Standard Model and which would also be detectable in the energy scale accessible to CDF II at the Main Injector. Predictions from models invoking new phenomena at the 100-200 GeV/ $c^2$  mass scale, the scale we will be exploring, have been made for Supersymmetry [1, 2, 3, 4, 5, 6], Technicolor [7], new U(1) symmetries [8], and Topcolor [9, 10, 11], for example.

The cross-sections for new states with masses in the 100-200 GeV/ $c^2$  range (*i.e.*, systems with total invariant mass in the 200-400 GeV/ $c^2$  range) are typically predicted to be in the range 10-1000 fb [2, 3, 4, 5, 6, 7, 8], so that with 2 fb $^{-1}$  detailed measurements are possible. The broad-band nature of the production process in  $\bar{p}p$  collisions is an advantage for searching as there is coupling to many different production processes: for example, in addition to Drell-Yan production, pairs of new particles such as charginos can be produced through gluons or through top decay.

#### 2.4.1.1 Impact of the Upgrade

Discovery relies heavily on a thorough understanding of the detector. Establishing a new and perhaps unexpected phenomena does not allow the luxury of systematic uncertainty; instead, there arise the most stringent requirements on confidence in all the parts of the measurement and the device. Two aspects are critical: the identification of objects that make up each signature, and the understanding of the calibration and resolution of the detector.

The objects for which we have already a good understanding of the efficiencies and fake-rates are those for which tracking is essential: electrons, muons, tau's,  $b$ 's, and photons (*i.e.*, a high confidence of the absence of a track), all in the central region. At Run II luminosities, the presence of multiple vertices will confuse the algorithms, with complications for object identification. The addition of the stereo capability to SVX and the strengthened COT stereo capabilities

will help enormously. An improved tracking system and improved calorimeter, along with its calibration, resolution, efficiency and coverage should also help to better understand  $\cancel{E}_T$  measurements.

Similarly, the energy scale and resolutions of the calorimeters, critical to the reconstruction of masses, are well understood in the central region, where the tracking information is used to calibrate the calorimeters. The integrated tracking and new plug calorimeter of the upgrade will extend the 'good' region where tracking is robust for  $e, \mu, \tau, \gamma$  and  $b$  identification, and will provide the calorimeter energy scale calibration, out to  $|\eta| = 2$ .

There are a number of other limitations in present searches that the upgrade will ameliorate. For instance, at present many channels with  $b$  decays are triggered on objects other than the  $b$ . Many signatures for new physics are tied to the heavy third generation, and thresholds can be lowered substantially by requiring a  $b$  at the trigger level. The  $\gamma bc\cancel{E}_T$  combination proposed by Kane [3] as a top squark (supersymmetric partner of a top quark) signature is a good example: at present the photon trigger threshold is set at 23 GeV, and in the absence of the SVT would have to be raised substantially in Run II, as we have no ability to trigger at present on the  $b$ . Other postulated states [2, 3, 7, 8] in the same mass region will have signatures of  $b\bar{b}$  or  $b\bar{c}$ , and will be triggerable.

In summary, the new plug calorimeter, new integrated tracking, and extended  $b$ -detection and triggering capability will provide a much larger and more uniform kinematic region in  $\eta$  and  $p_T$  for measurements of leptons,  $b$ -quarks, photons, jets, and  $\cancel{E}_T$ , while also providing the redundancy and cross checking that are crucial for precision calibration and the understanding of systematic effects.

#### 2.4.1.2 Current Situation and Plan

To date, many of the highest limits in direct searches for physics beyond the Standard Model come from CDF. Table 2.10 summarizes the current CDF limits on various new particles. In the sections below we describe our ongoing new phenomena searches and current results together with extrapolating the present performance to the upgrade. The following topics are covered: Supersymmetry, New Gauge Bosons  $Z'$  and  $W'$ , New Particles decaying to Dijets, Topcolor and the  $b$ -tagged Dijet Search, Leptoquarks, Compositeness, Massive Stable Particles, Technicolor, and

## CDF Exotic Particle Searches: Results and Run II Prospects

Searches	current CDF limit (Gev) Excluded region @ 95% C.L.		data set	run II (GeV) with 2 fb <sup>-1</sup>
W' → ev(SM)	< 652		1a (20 pb-1)	< 990
W' → WZ	<560 (ref. model excluded)	*	1a+1b (110 pb-1)	
Z' → ll (SM)	< 690	*	1a+1b (110 pb-1)	< 900
Zψ, Zη, Zχ, Z <sub>1</sub>	< 580,610,585,555	*	1a+1b (110 pb-1)	< 800
Z <sub>LR</sub> , Z <sub>ALRM</sub>	< 620,590	*	1a+1b (110 pb-1)	< 800
Axigluon → qq	200<M<930	*	1a+1b (103 pb-1)	< 1160
Techniro → dijet	250<M<500	*	1a+1b (103 pb-1)	200<M<770
E <sub>6</sub> Diquark → qq	280<M<350	*	1a+1b (103 pb-1)	200<M<570
topgluon Γ=.1M	200<M<550	*	1a (20 pb-1)	
topgluon Γ=.3M	210<M<450	*	1a (20 pb-1)	
topgluon Γ=.5M	200<M<370	*	1a (20 pb-1)	
Leptoquark (μq, τq)	< 180, 94 (scalar, β=1)	*	1a+1b (70 pb-1)	< 300
Pati-Salam LQ (Bs - eμ)	< 12900	*	1b (88 pb-1)	
Pati-Salam LQ (Bd - eμ)	< 18300	*	1b (88 pb-1)	
Composit. Scale (qqll)	3800(-), 2600(+) (ee)	*	1a+1b (110pb-1)	< 5000
q* (W+jet, γ+jet)	< 540	*	1a (20 pb-1)	< 820
q* → dijet	200<M<750	*	1a+1b (103 pb-1)	<820
massive stable ptl.	< 190 (col. tri. q)	*	1b (48 pb-1)	<300
gluino	< 180 (any m <sub>q</sub> ), < 230 (m <sub>g</sub> =m <sub>q</sub> )	#	1b (80 pb-1)	<200/<250
gaugino	χ <sub>1</sub> <sup>±</sup> < 68, χ <sub>2</sub> <sup>0</sup> < 68	#	1a+1b (100 pb-1)	<130
H <sup>±</sup>	< 130 (tanβ>100)	*	1b (88 pb-1)	

\* Current world best limit in direct search mode for the model.

# Same as \*, but D0 (also LEP1.5) has comparable limits.

Table 2.10: A summary of CDF's searches for physics beyond the standard model along with the prospects for Run II. update May 1st, 1996

**Charged Higgs Searches.** All quoted limits are at 95% confidence level (C.L.), unless explicitly stated otherwise. For simplicity we define 'mass reach' as the largest excluded mass at 95% C.L. [12, 13].

### 2.4.2 Supersymmetry

Supersymmetry (SUSY) [14] is a symmetry between bosons and fermions, and is the only known symmetry to provide the solution to a problem of the quadratic divergence of scalar mass parameters in the Standard Model. The experimental signatures of supersymmetry are complex, as all known fermions of the Standard Model have bosons as supersymmetric partners while all bosons acquire fermions as super-

partners, and in addition the symmetry is obviously broken, with possible additional large numbers of new fields. Due to the large number of free parameters, it is necessary to make further assumptions in the context of specific SUSY models. Two possibilities are that the breaking of SUSY is transmitted to the observable sector by gravitational interactions (supergravity models) [15, 16], or by gauge interactions [17]. Within these frameworks there are many variations, depending on specific assumptions of parameters. However general arguments can be made that the masses of the superpartners may lie in the region accessible by the Tevatron in Run II or Run III [1]. The Tevatron can explore a significant portion of the

parameter space using a number of possible signatures. The searches described below have been done using the framework of the MSSM, but are appreciably more general. Other searches, specific to certain models, are also now in progress.

One canonical signature is trilepton events, which would come from chargino-neutralino (*e.g.*,  $\tilde{\chi}_1^\pm \tilde{\chi}_2^0$ ) pair production with subsequent leptonic decays (*e.g.*,  $\tilde{\chi}_1^\pm \rightarrow l\nu\tilde{\chi}_1^0$  and  $\tilde{\chi}_2^0 \rightarrow \tilde{l}\tilde{\chi}_1^0$ ) [18]. Here  $\tilde{\chi}_1^0$  is assumed to be the lightest supersymmetric particle (LSP) and expected to escape from the detector ( $\cancel{E}_T$ ). Another signature is squark and gluino ( $\tilde{q}$  and  $\tilde{g}$ ) production followed by decays into the LSP and jets. Yet another is based on the Majorana nature of the gluino, which allows the gluino to decay into a chargino of either sign. One consequently searches for like-sign (LS) dilepton pairs from cases where a pair of gluinos have decayed into charginos of the same sign [19]. Searches for these three signatures, as well as a number of searches for the top squark (stop), predicted to be the lightest of the squarks, are underway with the Run I data.

More recently, there has been a flurry of activity on models in which radiative decays of neutralinos, either  $\tilde{\chi}_1^0$  [2, 3, 4, 5, 6] or  $\tilde{\chi}_2^0$  [3] are expected. These speculations are based on a single CDF  $ee\gamma\gamma\cancel{E}_T$  candidate event. Searches for sleptons, for charginos and neutralinos, the gravitino, and for the light stop are also underway in these scenarios.

### 2.4.2.1 The Trilepton Search

For this search pair-produced  $\tilde{\chi}_1^\pm \tilde{\chi}_2^0$  are assumed to decay as  $\tilde{\chi}_1^\pm \rightarrow l^\pm\nu\tilde{\chi}_1^0$  and  $\tilde{\chi}_2^0 \rightarrow l^+l^-\tilde{\chi}_1^0$ . Here  $\tilde{\chi}_1^0$  is assumed to be the lightest supersymmetric particle (LSP). The striking signature of these events is thus three isolated leptons plus  $\cancel{E}_T$  [18]. The CDF search is based on 100  $\text{pb}^{-1}$  data. Most of the events are from inclusive  $e$  and  $\mu$  triggers at  $p_T \sim 10$  GeV/ $c$ . The trilepton requirements are  $p_T(l_1) > 11$  GeV/ $c$  and  $p_T(l_{2,3}) > 5$  (4) GeV/ $c$  for  $e$  ( $\mu$ ), which is the same as in the previous analysis (based on 19  $\text{pb}^{-1}$ ) [20]. Eight events survive the selection, consistent with the SM background. A further cut of  $\cancel{E}_T > 15$  GeV is imposed to reduce the background. No trilepton event candidates are found, which is consistent with an expected background of  $0.4 \pm 0.1$  for four trilepton ( $eee$ ,  $ee\mu$ ,  $e\mu\mu$ ,  $\mu\mu\mu$ ) modes. Figure 2.28 shows the 95% C.L. upper limit on  $\sigma \cdot BR(\tilde{\chi}_1^\pm \tilde{\chi}_2^0 \rightarrow 3l + X)$  as a function of  $M_{\tilde{\chi}_1^\pm}$ , where “3l” is any 3-way combination of

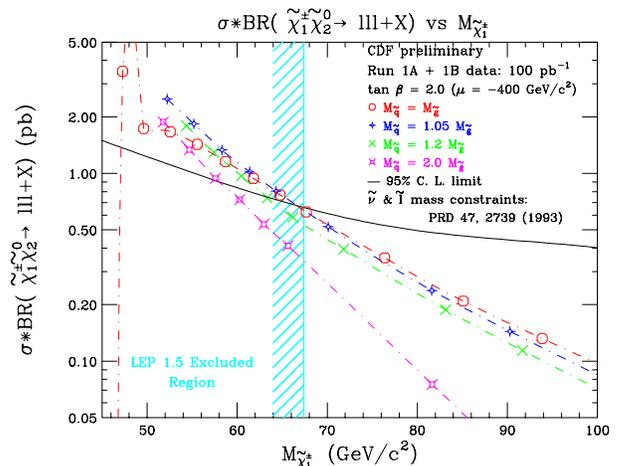


Figure 2.28:  $\sigma \cdot BR$  versus  $\tilde{\chi}_1^\pm$  mass for a representative point in MSSM parameter space ( $\tan\beta = 2$ ,  $\mu = -400$  GeV/ $c^2$ ).  $BR$  is the sum of the branching ratios for the four trilepton modes. The solid line is the 95% C.L. limit based on an observation of zero events. All points above the line are excluded.

$e$  and  $\mu$  as above. To obtain limits, CDF imposes a constraint inspired by supergravity models [21]. The CDF analysis [20] calculates slepton ( $\tilde{l}$ ) and sneutrino ( $\tilde{\nu}$ ) masses from  $\tan\beta$ ,  $M_{\tilde{g}}$ , and  $M_{\tilde{q}}$  using the renormalization group equations [22]. In these models, the chargino and neutralino have three-body decays. The CDF analysis excludes  $M_{\tilde{\chi}_1^\pm} < 68$  GeV/ $c^2$  (95% C.L.) at  $\tan\beta = 2$ ,  $M_{\tilde{q}} = M_{\tilde{g}}$  and  $\mu = -600$  GeV (the region of maximum experimental sensitivity). The CDF limit on  $\tilde{\chi}_1^\pm$  (68 GeV/ $c^2$ ) is comparable to the LEP1.5 result [23], assuming a heavy sneutrino. A limit on  $\sigma \cdot BR(\tilde{\chi}_1^\pm \tilde{\chi}_2^0 \rightarrow 3l + X)$  is also obtained: 0.6 pb (CDF) for a 70-GeV/ $c^2$  chargino. CDF also examines one particular supergravity model, a flipped SU(5) model [24]. In this model,  $M_{\tilde{l}_R} < M_{\tilde{\chi}_2^0} < M_{\tilde{l}_L}$ , so that the trilepton signal is nearly maximized via  $BR(\tilde{\chi}_2^0 \rightarrow \tilde{l}_R^\pm l^\mp) \sim 66\%$  ( $e$  and  $\mu$ ) and  $BR(\tilde{l}_R^\pm \rightarrow l^\pm \tilde{\chi}_1^0) = 100\%$ . However, the mass difference of  $\tilde{l}_R$  and  $\tilde{\chi}_1^0$  decreases as  $M_{\tilde{\chi}_1^\pm}$  increases, so that the total trilepton acceptance as a function of  $M_{\tilde{\chi}_1^\pm}$  becomes flat at about 5% at 60 GeV/ $c^2$  and falls off for  $M_{\tilde{\chi}_1^\pm} \gtrsim 75$  GeV/ $c^2$ . The limit on  $M(\tilde{\chi}_1^\pm)$  is 73 GeV/ $c^2$ .

Extrapolations of the chargino/neutralino search using the trilepton channel to higher integrated luminosities have been made by three groups [25, 26, 27]. Both Refs. [26, 27] assumed a large acceptance ( $|\eta| < 2.5$ ) for the leptons ( $e$  and  $\mu$ ), while coverage similar

to the current CDF detector is assumed in Ref. [25]. It should be noted that the selection cuts in Ref. [27] are optimized for the higher  $\tilde{\chi}_1^\pm$  mass region using high luminosity (*e.g.*, TeV33).

We take an extrapolation in Ref. [25] as a conservative estimate, because the tracking coverage is consistent with that by the SVX-II (5 layers) and COT system. We have revised the analysis in Ref. [25] by requiring  $\cancel{E}_T > 20$  GeV. The background cross section for  $DY/Z + X$  is expected to be 0.1 fb, while about 80% of 120-GeV/ $c^2$   $\tilde{\chi}_1^\pm$  events are accepted. The total background ( $DY/Z$ ,  $t\bar{t}$ , dibosons) becomes 0.5 fb which is the same level as in Ref. [26]. Taking into account the difference in the geometric coverage and details of the selection cuts, there are no obvious disagreements for the estimate of the total background. If we take the specific model used in the Run Ia and Ib analyses [20], the current mass limit can be extended to about 130 GeV/ $c^2$  with 2 fb $^{-1}$  of data in Run II.

Refs. [13, 26] studied the maximum mass reach in more generic MSSM models. In those studies, the coverage for leptons was assumed to be  $|\eta| < 2.5$ . The maximum chargino mass we can probe at 2 fb $^{-1}$  was found to be 210 GeV/ $c^2$  for a  $5\sigma$  significance above background. This is far above the maximum limit of 90 GeV/ $c^2$  from LEP-II ( $\sqrt{s} = 190$  GeV and  $\int \mathcal{L} dt = 500$  pb $^{-1}$ ) and is competitive to the limit of 248 GeV/ $c^2$  from NLC ( $\sqrt{s} = 500$  GeV and  $\int \mathcal{L} dt = 20$  fb $^{-1}$ ) [13].

#### 2.4.2.2 Classic Multi-jet Plus $\cancel{E}_T$ Search

Pairs of squarks and gluinos,  $\tilde{q}\tilde{q}$ ,  $\tilde{g}\tilde{g}$ , and  $\tilde{q}\tilde{g}$ , would be produced via the strong interaction. Depending on the relative masses of squarks and gluinos, production of  $\tilde{q}\tilde{q}$ ,  $\tilde{q}\tilde{g}$ , or  $\tilde{g}\tilde{g}$  may predominate. Direct decays of each  $\tilde{q}$  and  $\tilde{g}$  to quark +  $\tilde{\chi}^0$  (assumed to be the LSP) result in one and two quark jets respectively, while cascade decays through charginos and neutralinos may result in two or more additional jets. Events therefore always contain two jets, and most should contain three or more jets, in addition to missing energy. Two strategies are being followed: A high  $\cancel{E}_T$  plus three or more jet requirement to cover regions in supersymmetric parameter space in which squark production is dominant, and a more moderate  $\cancel{E}_T$  requirement in combination with a higher jet multiplicity for regions where gluino pair production has the highest cross-section.

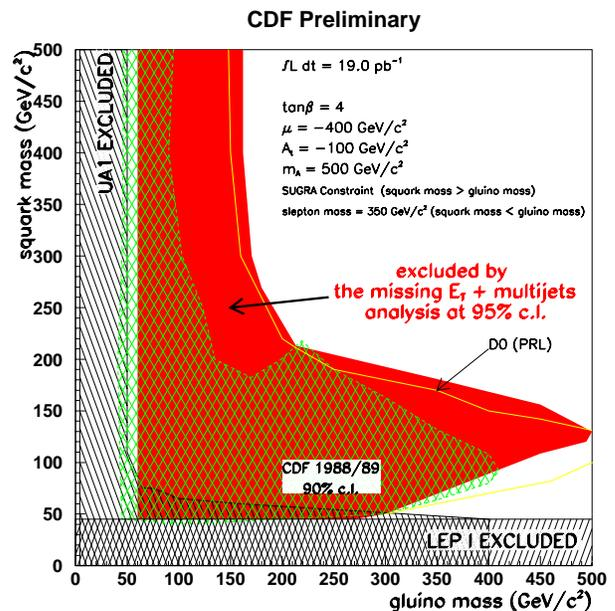


Figure 2.29: The 95% C.L. mass limit as a function of the squark and gluino mass values in jets plus  $\cancel{E}_T$  channels.

The Run Ia CDF search for multijet plus  $\cancel{E}_T$  events from SUSY requires 3 or more jets ( $E_T > 15$  GeV) and  $\cancel{E}_T > 60$  GeV. Additional cuts are imposed to reduce backgrounds from cosmic rays, mismeasured QCD multijet events,  $W/Z$  plus jet events, and other sources, to a reasonable level. The removal of  $W/Z$  plus jets backgrounds requires rejection of events with electrons or muons. In the final data sample there are 23 events with 3 or more jets over an estimated background of  $35.1^{+11.6}_{-9.1}$  (stat)  $^{+15.3}_{-5.5}$  (sys) and 6 events with 4 or more jets over an estimated background of  $8.5^{+4.2}_{-3.0}$  (stat)  $^{+2.6}_{-1.9}$  (sys). The background estimate contains  $W$  and  $Z$  leptonic, and top semileptonic decays. The  $W$  and  $Z$  hadronic decay backgrounds (lepton not observed) are normalized directly to the data, using multijet events in which a lepton is observed. We conclude that no significant excess is observed, and set a conservative upper limit on potential SUSY contributions by assuming a zero background contribution from QCD mismeasurement. The region of the  $M_{\tilde{q}} - M_{\tilde{g}}$  plane which is excluded by this analysis is shown in Figure 2.29. For arbitrary  $M_{\tilde{q}}$  the data require  $M_{\tilde{g}} > 160$  GeV/ $c^2$  and for  $M_{\tilde{g}} \approx M_{\tilde{q}}$  we deduce  $M_{\tilde{g}} > 220$  GeV/ $c^2$ .

The larger data samples of Run Ib and Run II will allow proportionally better determination of the backgrounds. However, since the analysis is back-

ground dominated, better limits will be obtained by tightening analysis cuts and perhaps fitting the shape of the  $\cancel{E}_T$  spectrum.

For  $0.1 \text{ fb}^{-1}$ , we need to reduce the background substantially. CDF used cuts of  $\cancel{E}_T > 60 \text{ GeV}$  and  $N_{jet}(E_T > 15 \text{ GeV}) \geq 3$  in the Run Ia analysis. We have revised this analysis with cuts of  $\cancel{E}_T > 80 \text{ GeV}$  and  $N_{jet}(E_T > 20 \text{ GeV}) \geq 4$ . The other cuts on lepton veto fake  $\cancel{E}_T$  due to mismeasured jet *etc.* remain the same. With the new cuts, our expectation of the background cross section is  $0.16 \text{ pb}$ . The  $1.64\sigma$  significance above background for  $0.1 \text{ fb}^{-1}$  is  $0.07 \text{ pb}$  (or 7 events). Therefore, we find the 95% C.L. limit on the gluino mass of  $270 \text{ GeV}/c^2$  if  $M_{\tilde{q}} \simeq M_{\tilde{g}}$  for a specific choice of SUSY model [13].

The dominant background sources are  $t\bar{t}$ ,  $W$  and  $Z$  events. Further reduction of background can be reduced by requiring  $E_{Tj_1} + E_{Tj_2} + \cancel{E}_T > 300 \text{ GeV}$  [26]. The total background is then estimated to be  $40 \text{ fb}$ . With more generic SUSY models, the maximum possible reach (95% C.L. upper limit is  $\sigma = 7.3 \text{ fb}$ ) can be over  $400 \text{ GeV}/c^2$  [26].

Some help from theorists may be forthcoming when recent NLO calculations of squark pair production, which show cross-sections approximately double those of the leading order calculations, are extended to squark/gluino and gluino/gluino production.

### 2.4.2.3 Search for Gluino Cascade Decays in the Dilepton Channel

Light gluinos ( $M_{\tilde{g}} \lesssim 70 \text{ GeV}/c^2$ ) decay preferentially into a quark-antiquark pair and an LSP. However, the decays into a chargino will dominate as soon as they are kinematically allowed [28]. Since the gluino is a Majorana particle, the charge of the chargino can be either  $+1$  or  $-1$  in a gluino decay. For example,  $\tilde{g} \rightarrow \tilde{u}^* \bar{u} \rightarrow (d\tilde{\chi}_1^+) \bar{u}$  and  $\tilde{g} \rightarrow u \tilde{u}^* \rightarrow u + (d\tilde{\chi}_1^-)$  will equally be seen, if  $M_{\tilde{q}} > M_{\tilde{g}} > M_{\tilde{\chi}_1^\pm}$ . A subsequent chargino decay can yield a lepton, a neutrino and an LSP (*e.g.*,  $\tilde{\chi}_1^\pm \rightarrow l^\pm \nu \tilde{\chi}_1^0$ ). Thus, a dilepton pair (OS or LS) + multijets +  $\cancel{E}_T$  is a signature of gluino pair production. Moreover, LS dileptons are a distinctive signature with small SM backgrounds[19]. The dilepton analysis complements the classic  $\cancel{E}_T$  plus multijet analyses: while the  $\cancel{E}_T$  plus multijet analysis is degraded by cascade decays<sup>1</sup>, the dilepton analysis is

<sup>1</sup>Cascade decays reduce the amount of  $\cancel{E}_T$  produced in a gluino or squark decay (compared to the direct decay into LSP) and thus the detection efficiency in the  $\cancel{E}_T$  based searches.

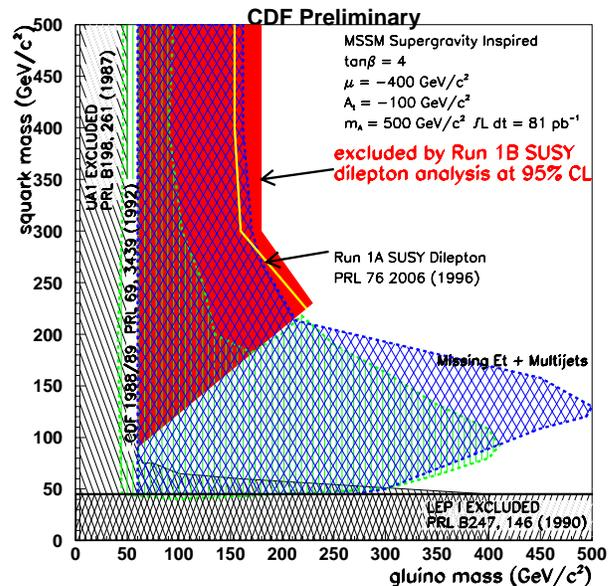


Figure 2.30: The 95% C.L. mass limit as a function of squark and gluino mass values from the LS dilepton + jets +  $\cancel{E}_T$  channel.

based upon them.

In Run Ia ( $19 \text{ pb}^{-1}$ ), we did not apply the LS requirement [29]. The dilepton requirements are  $p_T(l_1) > 12 \text{ GeV}/c$  ( $|\eta_e| < 1.1$  or  $|\eta_\mu < 0.6$ ) and  $p_T(l_2) > 11 \text{ GeV}/c$  ( $|\eta_e| < 2.4$  or  $|\eta_\mu < 1.0$ ). Electron or muon pairs with opposite charge with  $70 \text{ GeV}/c^2 < M_{ll} < 105 \text{ GeV}/c^2$  are removed. In addition, we require: (a) 2 or more jets ( $E_T > 15 \text{ GeV}$ ) in  $|\eta| < 2.4$  with at least one of them in the central region ( $|\eta| < 1.1$ ); (b)  $\cancel{E}_T > 25 \text{ GeV}$ ; (c)  $I(l_1) + I(l_2) < 8 \text{ GeV}$ , where  $I$  is a measure of the amount of energy surrounding each lepton using a combination of calorimeter and tracking information; (d)  $\Delta\phi_{ll} < 60^\circ$  or  $60^\circ < \Delta\phi_{ll} < 120^\circ$  if  $p_T(ll) < 40 \text{ GeV}/c$  or  $\Delta\phi_{ll} < 120^\circ$  if  $p_T(ll) < 20 \text{ GeV}/c$ . Only one candidate event (a  $\mu^+\mu^-$  event) is observed. In comparison, the expected number of background events from SM processes is  $2.39 \pm 0.63(\text{stat})_{-0.42}^{+0.77}(\text{sys})$ . We have set limits on gluino and squark production in the MSSM. For squark mass equal to the gluino mass, we exclude gluinos up to  $224 \text{ GeV}/c^2$ . For heavy squarks,  $M_{\tilde{q}} = 400 \text{ GeV}/c^2$ , we exclude gluinos up to  $154 \text{ GeV}/c^2$  ( $\tan\beta = 4.0$  and  $\mu = -400 \text{ GeV}/c^2$ ) [29].

For the Run Ib data ( $81 \text{ pb}^{-1}$ ), we have repeated the Run Ia dilepton analysis without the  $\Delta\phi_{ll}$  and  $p_T(ll)$  cuts, but with the LS requirement and lower

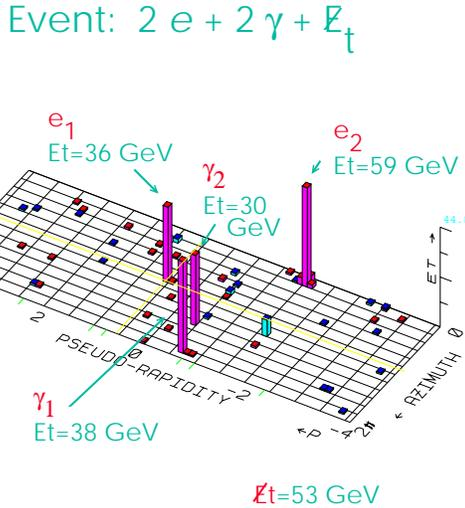


Figure 2.31: The Lego plot of the  $ee\gamma\gamma\cancel{E}_T$  candidate event.

lepton  $p_T$  cuts ( $p_T(l_1) > 11$  GeV/ $c$  and  $p_T(l_2) > 5$  GeV/ $c$ ). It should be noted that the LS requirement reduces the signal events by a factor of four. Lowering the lepton  $p_T$  cuts was necessary to recover the loss of acceptance. In a preliminary analysis, we observed two events, where the expected number of background events was  $1.29 \pm 0.62(\text{stat}) \pm 0.35(\text{sys})$ : dominant sources are 0.58 events from  $t\bar{t}$ , 0.46 events from DY, and 0.22 events from  $W$  plus a misidentified additional lepton. The 95% C.L. upper limits on gluino and squark masses were determined in the same manner as in the Run Ia analysis [29]. The resultant limits as a function of the squark and gluino mass values are shown in Figure 2.30. For squark mass equal to the gluino mass, we exclude gluinos up to 230 GeV/ $c^2$ . For heavy squarks,  $M_{\tilde{q}} = 400$  GeV/ $c^2$ , we exclude gluinos up to 180 GeV/ $c^2$  ( $\tan\beta = 4.0$  and  $\mu = -400$  GeV/ $c^2$ ). We are investigating additional cuts to improve the signal-to-background ratio.

The LS dilepton analysis is complementary to the classic  $\cancel{E}_T$  + jets analysis and has very little background. The striking signature of LS dilepton + jets +  $\cancel{E}_T$  makes this analysis ideal for Run II (and Run III). We also note that two analyses can be combined to improve the mass limits. This is underway for Run Ib data.

#### 2.4.2.4 Radiative Decays of Neutralinos

One can interpret the signature  $ee\gamma\gamma\cancel{E}_T$  of one event in our data, shown in Figure 2.31, as a possible supersymmetry candidate. A search is underway for similar events in the diphoton channel; this is the dominant channel in scenarios in which the gravitino is the LSP [5] as well in the slepton or chargino production scenarios [2, 3, 4, 6]. A search for the light stop in the signature  $\gamma + b + jet + \cancel{E}_T$  is also underway in these scenarios, as are other searches involving photons plus missing  $E_T$  and/or leptons. In all of these scenarios the ability to identify a  $b$  quark is a powerful tool (for example, most stop signatures involve  $b$  quarks); in Run II the SVT will allow us the ability to trigger on the  $b$  allowing lower photon or lepton thresholds, and the extended coverage and improved pattern recognition of the integrated tracking system will substantially increase the tagging efficiency.

#### 2.4.2.5 The Light Stop Quark

One of two top squarks (stops) may have a mass significantly lower than other squarks. Here,  $\tilde{t}_1$  is the lighter stop. The cross section for stop pair production is expected to be an order of magnitude smaller than the production of ‘ordinary’ top quark pairs for equal masses. For example, a stop with mass around 110 GeV/ $c^2$  is expected to have about the same production rate as the 175 GeV/ $c^2$  top quark. Two decay modes for the light stop which could be detectable at the Tevatron [13]: ( $M_{\tilde{t}_1} < M_{top}$ ): (a)  $\tilde{t}_1 \rightarrow \tilde{\chi}_1^+ b$ ; (b)  $\tilde{t}_1 \rightarrow \tilde{\chi}_1^0 c$ . Several searches are underway for the stop using Run I data.

A Monte Carlo study for the mass reach of the stop in Run II, has been made and described in Ref. [13]. The  $5\sigma$  mass limit was found to be 150 GeV/ $c^2$  for 2 fb $^{-1}$ .

#### 2.4.3 New Gauge Bosons $Z'$ and $W'$

Heavy neutral gauge bosons in addition to the  $Z^0$ , generically denoted as  $Z'$ , occur in any extension of the Standard Model that contains an extra U(1) after symmetry breaking. For example, in one model with  $E_6$  as the grand unified gauge group [30] there exists a  $Z_\psi$  from the symmetry breaking  $E_6 \rightarrow SO(10) \times U(1)_\psi$  and a  $Z_\chi$  from the symmetry breaking  $SO(10) \rightarrow SU(5) \times U(1)_\chi$ . Finally the SU(5) symmetry breaks to recover the Standard Model:

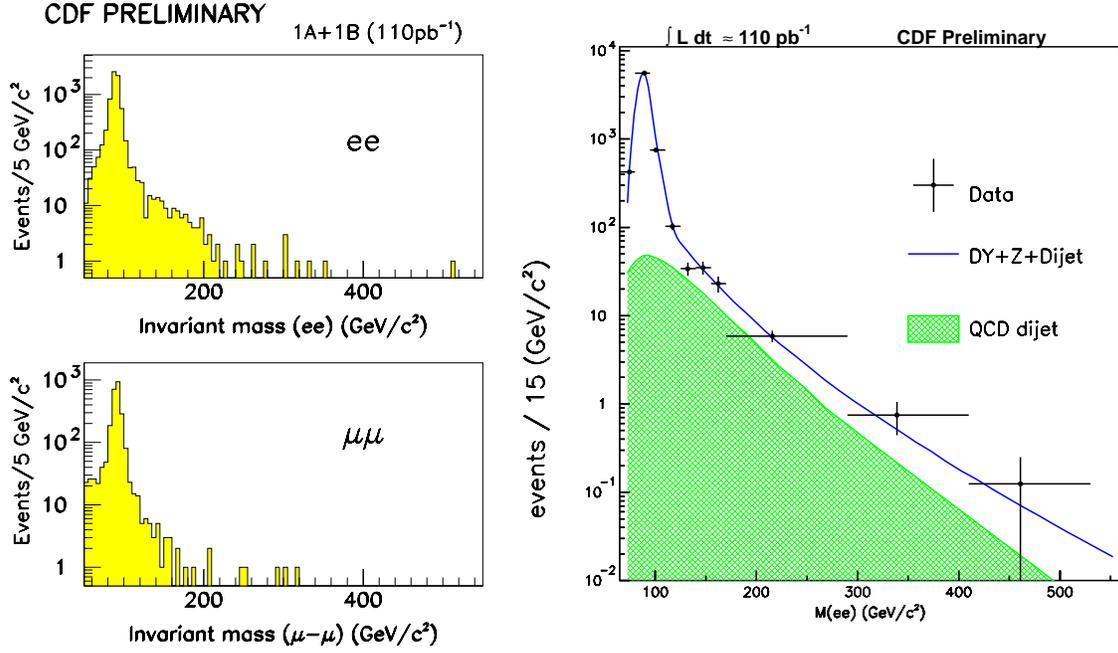


Figure 2.32: Left: The dielectron and dimuon invariant mass distributions for the  $Z'$  search data sample. Right: The dielectron invariant mass distributions compared to background predictions.

$SU(5) \rightarrow SU(3)_C \times SU(2)_L \times U(1)_Y$ . In superstring inspired  $E_6$  models there exists a  $Z_\eta$  which is the linear combination  $Z_\eta = \sqrt{3/8}Z_\chi + \sqrt{5/8}Z_\psi$ .

In each running period (88/89, Run Ia, and Run Ib), we have searched for  $Z' \rightarrow ll$  and set the world's best mass limit. Most recently, we have analysed  $110 \text{ pb}^{-1}$  of Run Ia and Ib data in both dimuon and dielectron decay modes. Figure 2.32 shows the invariant mass distributions of dimuons and dielectrons in the  $Z'$  search data sample and the comparison of data with background predictions. From this analysis, we set the current best limit of  $M_{Z'} > 690 \text{ GeV}/c^2$  for Standard Model couplings.

This experimental limit can be compared with specific models. For example, we set the lower mass limits for  $Z_\psi$ ,  $Z_\eta$ ,  $Z_\chi$ ,  $Z_I$ ,  $Z_{LR}$  and  $Z_{ALRM}$  to be 580, 610, 585, 555, 620, and 590  $\text{GeV}/c^2$ , respectively. Extrapolating to Run II we predict that the mass reach can be extended to 900  $\text{GeV}/c^2$ , assuming Standard Model couplings, and to about 800  $\text{GeV}/c^2$  for the specific cases mentioned above, assuming  $\sqrt{s} = 1.8 \text{ TeV}$ . (Extrapolated mass limits are higher by approximately 100  $\text{GeV}/c^2$  if we assume  $\sqrt{s} = 2.0 \text{ TeV}$ .) See Figure 2.33.

Heavy W bosons,  $W'$ , occur in some extended gauge models, for example, the left-right symmet-

ric model [31] of electroweak interactions  $SU(2)_R \times SU(2)_L \times U(1)_Y$ . CDF has searched for  $W' \rightarrow l\nu$  in the electron and muon channels [32, 33]. The analysis of Run Ia electron data yielded a limit of  $M_{W'} > 652 \text{ GeV}/c^2$ , assuming Standard Model couplings and that the decay  $W' \rightarrow WZ$  is not allowed. The analysis of  $W' \rightarrow e\nu$  and  $\mu\nu$  Run Ib data is in progress. Extrapolating to a Run II luminosity of  $2 \text{ fb}^{-1}$  we predict that the mass reach can be extended to 990  $\text{GeV}/c^2$  in the  $W' \rightarrow e\nu$  mode. See Figure 2.33.

We have also performed a new search for  $W'$  decaying to  $WZ$  [34] and have excluded a range region of mass vs. mixing angle ( $\xi$ ) space. This region is shown on the left in Figure 2.33. Searches for  $W' \rightarrow tb$  and  $W' \rightarrow WH$  are in progress.

We have also searched for  $Z' \rightarrow q\bar{q}$  and  $W' \rightarrow q\bar{q}$  in the dijet channel using the entire run Ia and Ib dataset. We set upper limits on the cross section which are currently larger than the theoretical prediction of  $Z'$  and  $W'$  production cross sections which assumes Standard Model couplings, in all dijet mass regions. Extrapolating the cross section limits to  $2 \text{ fb}^{-1}$  we expect to have a mass reach of approximately 720  $\text{GeV}/c^2$  for both  $Z'$  and  $W'$  from the dijet decay mode.

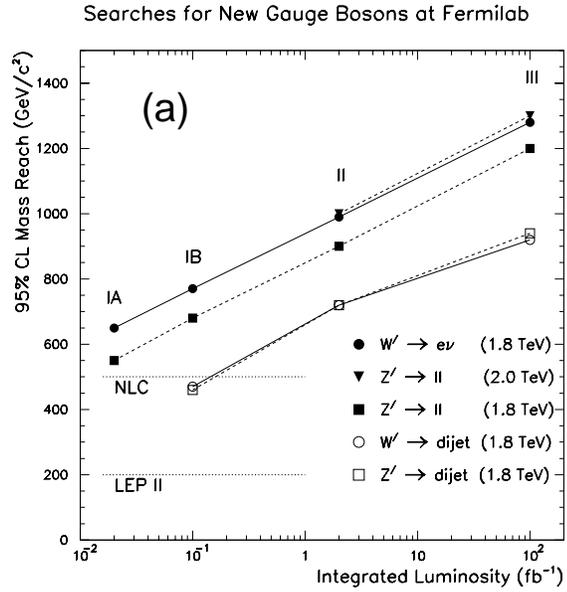
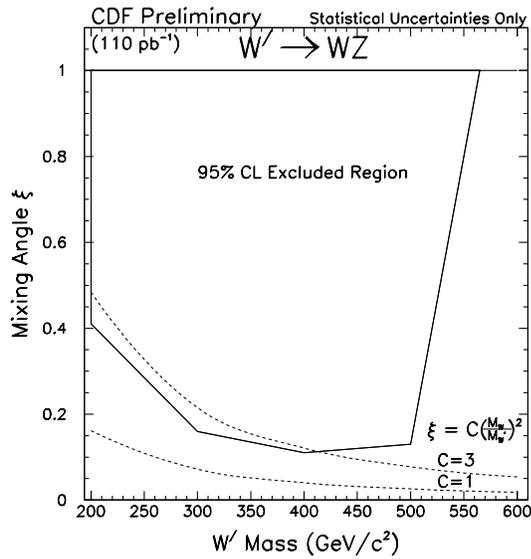


Figure 2.33: Left: Limits are shown for  $W' \rightarrow WZ$ . Right: The expected mass reach, defined as the 95% C.L. lower limit on the mass vs. integrated luminosity at the Tevatron for searches for new gauge bosons.

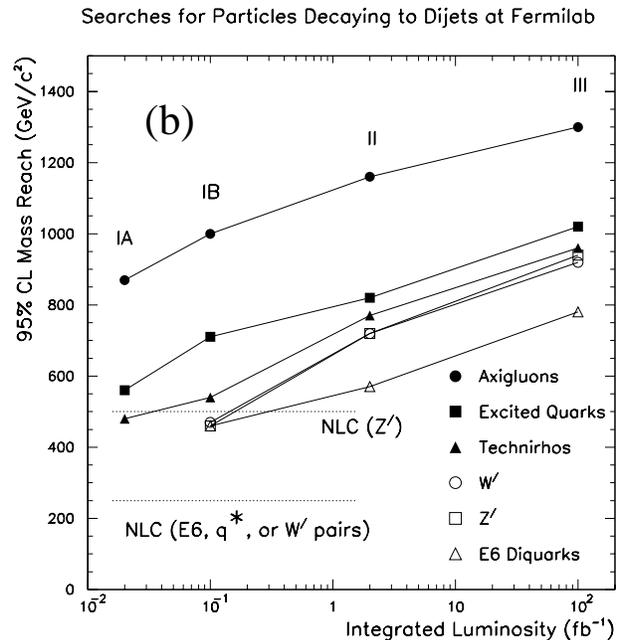
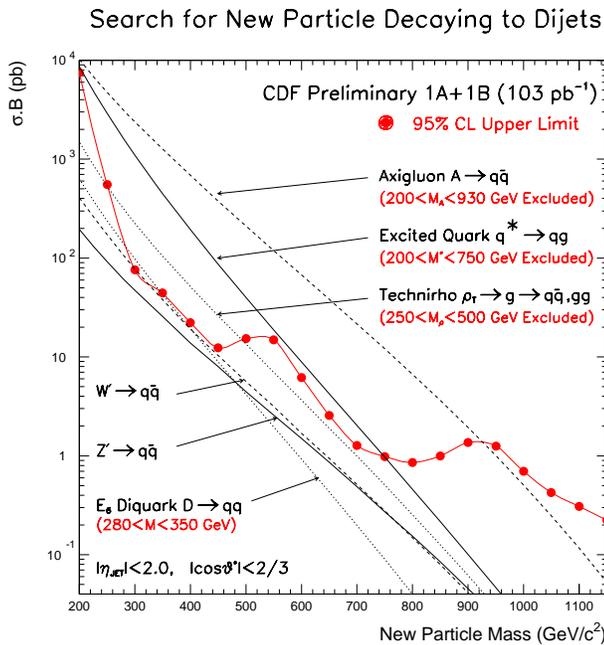


Figure 2.34: Left: The cross section times branching ratio limits as a function of dijet mass, as well as the resulting limits for various specific models. Right: The expected mass reach, defined as the 95% C.L. lower limit on the mass, vs. integrated luminosity at the Tevatron for searches for new particles decaying to dijets.

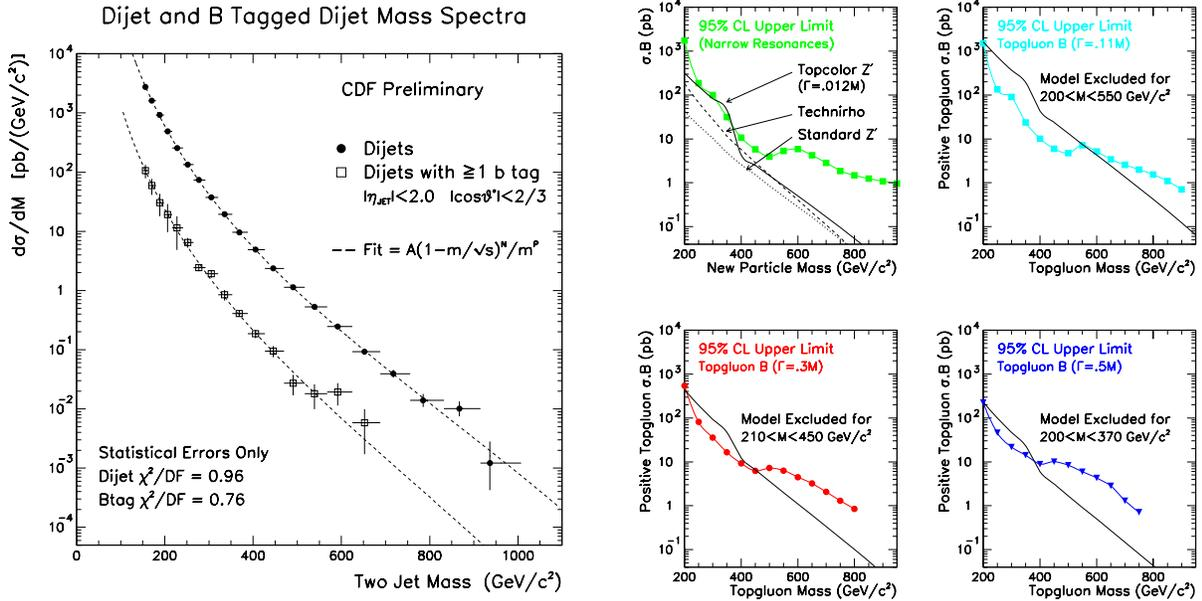


Figure 2.35: Left: The invariant mass distribution of  $b$ -tagged dijets. Right: The limits on  $Z'_{TopC}$  and topgluons of various widths.

## 2.4.4 New Particles decaying to Dijets

Many theories predict particles which decay to dijets. These would appear as bumps in the dijet mass spectrum. The existence of a larger chiral color group,  $SU(3)_L \times SU(3)_R$ , would lead to massive color-octet axial vector gluons, axigluons, which would be produced and decay strongly giving a very large cross section times branching ratio to dijets [35, 36]. A recent technicolor model [37, 38] predicts a color octet technirho ( $\rho_T$ ) which couples to  $q\bar{q}$  and  $gg$  via a gluon. If quarks are composite particles, then excited states of composite quarks are expected and couple to  $gg$  as discussed in section 2.4.7. New gauge bosons,  $W'$  and  $Z'$ , in addition to coupling to leptons as discussed in section 2.4.3, would produce dijet mass bumps. Superstring-inspired  $E_6$  models predict the existence of many new particles [40] including a color triplet scalar diquark  $D(D^c)$  with charge  $-(+)\frac{1}{3}$  which couples to  $\bar{u}d(ud)$ . Continuing our Run Ia search [41], in Run Ib we have searched for resonances and set limits on these theories. At high mass, the data are consistently higher than the QCD Monte Carlo prediction. This issue is discussed in more detail in the QCD

section of this document. To search for high mass resonances, we compare the data with a curve obtained from a fit to the data. The cross section times branching ratio limits which we derive are shown as a function of dijet mass in Figure 2.34, as well as the resulting limits for various specific models. The predictions for Run II are shown on the right in Figure 2.34 and listed in Table 2.10.

## 2.4.5 Topcolor Theory and the $b$ -tagged Dijet Search

The large mass of the top quark suggests that the third generation may be special. This has motivated the Topcolor model [9, 10, 11] which assumes that the top mass is large mainly because of a dynamical  $t\bar{t}$  condensate generated by a new strong dynamics coupling to the third generation. It predicts massive color-octet bosons, topgluons ( $B$ ), and a new gauge boson,  $Z'_{TopC}$ , from an additional  $U(1)$  symmetry. Both of these new particles couple largely to  $b\bar{b}$  and  $t\bar{t}$ . Using CDF's  $b$ -tagging capabilities we have searched for topgluons  $B$  and  $Z'_{TopC}$  in the  $b\bar{b}$  channel. Figure 2.35 shows the invariant mass distri-

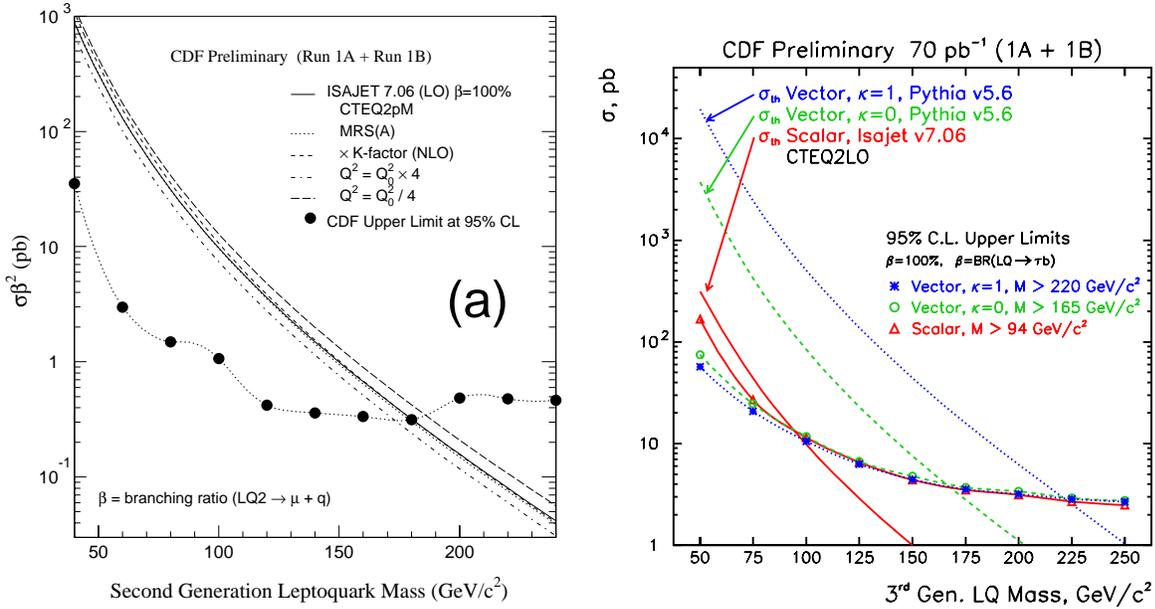


Figure 2.36: Left: The limit on  $\sigma \cdot \beta^2$  is shown as a function of LQ2 mass. Right: The limit on  $\sigma \cdot \beta^2$  is shown as a function of LQ3 mass.

bution of  $b$ -tagged dijets and the limits on  $Z'_{TopC}$  and topgluons of various widths. A search is also underway in the  $t\bar{t}$  mass distribution, as described in the top section. We estimate that a  $Z'_{TopC}$  decaying into  $t\bar{t}$  can be discovered (5 sigma) in run II if its mass is less than 900 GeV.

## 2.4.6 Leptoquarks

Leptoquarks belong to a class of particles carrying both color and lepton quantum numbers which mediate transitions between quarks and leptons. Leptoquarks do not exist within the Standard Model but appear in many SM extensions which predict a symmetry between quarks and leptons at a fundamental level [42, 43, 44]. At CDF we have performed two qualitatively different searches for leptoquarks which will be described in the following two subsections.

### 2.4.6.1 Direct search for pair produced leptoquarks

Leptoquark masses and coupling strengths are severely constrained by experimental bounds on rare processes, so one has to make the following assumptions about the properties of leptoquarks and their

couplings to allow masses which are directly observable in collider experiments:

1. to evade mass bounds from proton decay, lepton and baryon number have to be conserved;
2. to prevent leptoquark-induced FCNC, leptoquarks are generally assumed to link, through an unknown coupling strength, quark and lepton multiplets of the same generation, and
3. to avoid LQ contributions to the helicity suppressed  $\pi \rightarrow e\nu$  decay, the couplings have to be chiral.

We have searched for pair production of scalar leptoquarks in the dilepton plus dijet channels. In the 88/89 run, we set a first generation leptoquark (LQ1) mass limit of  $M_{LQ1} > 113 \text{ GeV}/c^2$  for  $\beta = 100\%$  and  $M_{LQ1} > 80 \text{ GeV}/c^2$  for  $\beta = 50\%$ , where  $\beta$  is the branching ratio for a leptoquark decaying to a charged lepton and quark. Since then, HERA has improved the first generation limits. But their limits depend on the (unknown) coupling strength  $\lambda$ , unlike at hadron colliders where because the leptoquarks are produced strongly there is only a weak dependence between the production cross section and  $\lambda$ . In Run

In Ia we set the world's best limit on second generation scalar leptoquarks (LQ2) and have subsequently improved it with Run Ib data. The current best limit is  $M_{LQ2} > 180 \text{ GeV}/c^2$  for  $\beta = 100\%$  and  $M_{LQ2} > 140 \text{ GeV}/c^2$  for  $\beta = 50\%$ . Figure 2.36 shows the limit on  $\sigma \cdot \beta^2$  as a function of LQ2 mass. Extrapolating to Run II, we expect to extend the second generation mass reach to  $300 \text{ GeV}/c^2$ .

Just recently we have completed a search for third generation leptoquarks (LQ3) into the  $\tau\tau$  plus dijet final state where one  $\tau$  decays leptonically and the other hadronically. For scalar leptoquarks we set a limit at  $M_{LQ3} > 94 \text{ GeV}/c^2$ . We also considered vector leptoquarks with "anomalous chromomagnetic moments" parametrized by  $\kappa$ . For this type of leptoquark assuming  $\beta = 1$ , the limits are  $M_{LQ3} > 165 \text{ GeV}/c^2$  and  $M_{LQ3} > 222 \text{ GeV}/c^2$  for  $\kappa=0$  and  $\kappa = 1$  respectively. See the right plot in Figure 2.36.

#### 2.4.6.2 Search for the decays $B_s^0 \rightarrow e\mu$ and $B_d^0 \rightarrow e\mu$

Within the Pati-Salam model [42], which is based on the group  $SU(4)_c$ , lepton number is regarded as the fourth "color". At some high-energy scale, the group  $SU(4)_c$  is spontaneously broken to  $SU(3)_c$ , liberating the leptons from the influence of the strong interaction and breaking the symmetry between quarks and leptons. This model predicts a heavy spin-one gauge boson with non-chiral couplings called the Pati-Salam boson. The lepton and quark components in this kind of leptoquark are not necessarily from the same generation as pointed out in [45]. This would make decays like  $B_s^0 \rightarrow e\mu$  and  $B_d^0 \rightarrow e\mu$  possible. Setting limits on the branching ratio of these rare processes can probe masses in the multi-TeV range, *i.e.*, masses not accessible directly. We have searched for the decays  $B_s^0 \rightarrow e\mu$  and  $B_d^0 \rightarrow e\mu$  using  $\approx 90 \text{ pb}^{-1}$  of Run Ib data. We find no  $B_d^0$  candidates in a mass window of  $5.174\text{-}5.384 \text{ GeV}/c^2$  and one  $B_s^0$  candidate in a mass window of  $5.270\text{-}5.480 \text{ GeV}/c^2$ . We set limits at  $\text{Br}(B_s^0 \rightarrow e\mu) < 1.8(2.3) \times 10^{-5}$  and  $\text{Br}(B_d^0 \rightarrow e\mu) < 3.3(4.4) \times 10^{-6}$  at 90(95)% C.L. after systematic uncertainties have been included. From this we derive a limit on the mass of a certain Pati-Salam leptoquark of  $12.8$  ( $12.1$ )  $\text{TeV}/c^2$  at 90(95)% C.L. for the  $B_s$  and  $19.6$  ( $18.3$ )  $\text{TeV}/c^2$  at 90(95)% C.L. for the  $B_d$ .

The Run II prospects for this analysis are promising. The new Silicon Vertex detector SVX-II, which

is crucial for this kind of analysis, will have twice the acceptance of the current SVX'. In addition the ability to trigger on displaced vertices from  $b$  decays with the SVT will have a big impact, allowing us access B-mesons with lower momentum. For the current analysis the  $\mu p_T$  and electron  $E_T$  trigger thresholds are  $3 \text{ GeV}/c$  and  $5 \text{ GeV}$  respectively, resulting in a mean B-meson  $p_t$  of  $\approx 13 \text{ GeV}/c$ . Since the B-meson cross section is falling rapidly with  $p_T$  one gains by lowering the momentum threshold (by lowering the threshold from  $12$  to  $6 \text{ GeV}/c$  one gains a factor of  $\approx 10$ ).

#### 2.4.7 Compositeness

The Standard Model has a large number of parameters and particles. One way to simplify is to consider a possibility that these parameters and particles are composed of a smaller and simpler set. If quarks and leptons are composite particles we expect four-fermion contact interactions [46] to modify the quark and lepton production cross sections at high transverse momentum. Excited states [47] would also be expected and can be searched for in the invariant mass spectrum.

We have searched for an excess of events in the inclusive jet cross section which could result from the four-quark contact interaction. An excess of events has been observed in the Run Ia data [48]. The Run Ib data are now being analysed: preliminary results show good agreement with the Run Ia results. However, we should note that inclusion of our data in a global fit with those from other experiments may yield a consistent set of PDFs that accommodate the high- $E_T$  excess within the scope of QCD [49, 50, 51].

If quarks and leptons are both composite and share constituents, then effective contact interactions arise between them at low energies [46]. We have searched for the quark-lepton contact interaction in the dielectron and dimuon channels by looking for an excess of high mass dileptons compared to the Drell-Yan prediction. From the 1988-89 data we had set limits on the lepton-quark compositeness scale of  $\Lambda^- > 2.2 \text{ TeV}$  and  $\Lambda^+ > 1.7 \text{ TeV}$  for electrons [52], where  $-(+)$  corresponds to the constructive (destructive) interference with the dominant up-quark contribution to the cross section. In the muon channel, the limits are  $\Lambda^- > 1.6 \text{ TeV}$  and  $\Lambda^+ > 1.4 \text{ TeV}$  [53]. Preliminary results using the Run Ib data in the dielectron channel extend the limits on the compositeness scale

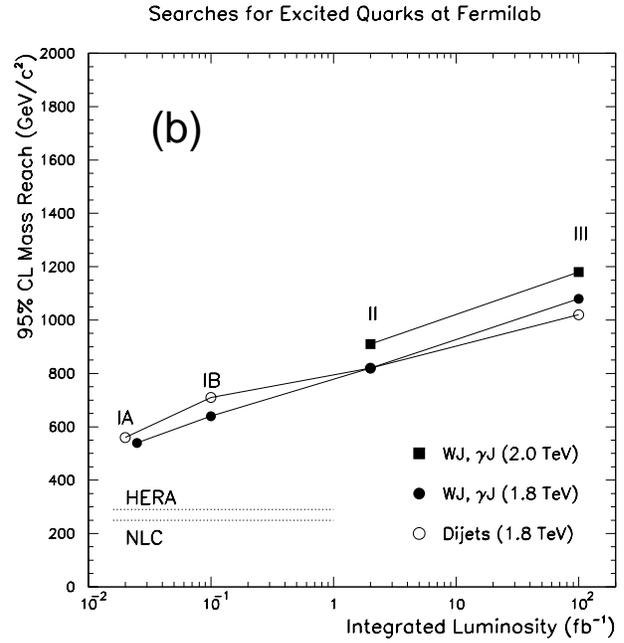
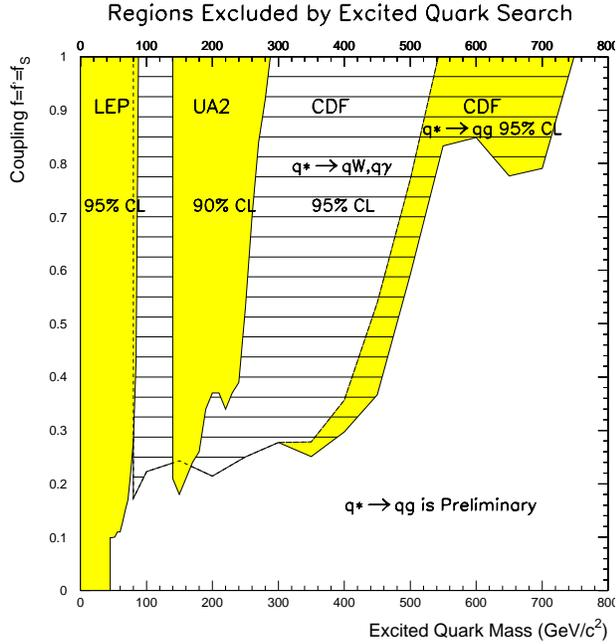


Figure 2.37: Left: The mass regions currently excluded by the dijet  $q^*$  search. Right: The expected  $q^*$  mass reach, defined as the 95% C.L. lower limit on the mass, plotted vs. integrated luminosity.

to  $\Lambda^- > 3.8$  TeV and  $\Lambda^+ > 2.6$  TeV. In Run II we expect to be able to explore up to limits of approximately 5 TeV.

Excited states of composite quarks, denoted  $q^*$ , have been searched for at UA2 [54] and CDF [55]. They would be produced singly by quark gluon fusion and could decay to a common quark and any gauge boson ( $g$ ,  $\gamma$ ,  $W$  or  $Z$ ) [47]. Using the photon + jet and  $W$  + jet channels in the Run Ia data, we have excluded the mass region below  $540$   $\text{GeV}/c^2$  for the simplest model of  $q^*$  [55]. We have also searched for  $q^*$  decaying into a dijet mode ( $q^* \rightarrow qg$ ) with  $70$   $\text{pb}^{-1}$  of Run Ia and Ib data, and we have excluded the mass range between  $200$  and  $600$   $\text{GeV}/c^2$  for the simplest model of  $q^*$  (Figure 2.34). Extrapolating to a Run II luminosity of  $2$   $\text{fb}^{-1}$  we predict that the  $q^*$  mass reach can be extended to  $820$   $\text{GeV}/c^2$  in each of these decay modes. See Figure 2.37 and Table 2.10.

Currently the best limit for excited states of composite leptons,  $l^*$ , is set by a LEP experiment. The lower limit is  $45$   $\text{GeV}/c^2$  for pair production and  $90$   $\text{GeV}/c^2$  for single production. Recently, we have started an analysis searching for  $l^*$  in the  $e\gamma$  final state. We expect that we will explore up to a mass limit of several hundred GeV with the current data, and as for the  $q^*$  search, the mass reach will be sub-

stantially extended in Run II.

#### 2.4.8 Massive Stable Particles

Massive stable particles are possible features of several theories for physics beyond the standard model including supersymmetry, mirror fermions, technicolor, and compositeness. We have searched in the 88/89 data for heavy stable charged particles [56, 57] based upon their expected high transverse momenta, relatively low velocities (via time-of-flight), and muon-like penetration of matter. We obtained upper limits on the cross-section for the production of heavy stable particles as a function of their mass. This can be translated into a mass limit from the cross-section for any particular theory and varies from about  $140$   $\text{GeV}/c^2$  for color triplets to  $255$   $\text{GeV}/c^2$  for color decuplets as shown in Figure 2.38b. This analysis is currently being extended using Run I data. Rather than using time-of-flight, the analysis takes advantage of the large ionization depositions,  $\frac{dE}{dx}$ , expected for massive particles, with measurements in both the SVX and in the outer tracker (CTC for Run I). For example, see Figure 2.38a. Using half of the Run Ib data, we have obtained a preliminary limit of  $190$   $\text{GeV}/c^2$  for color triplets. The extrapolations to Run II are shown in Figure 2.38b.

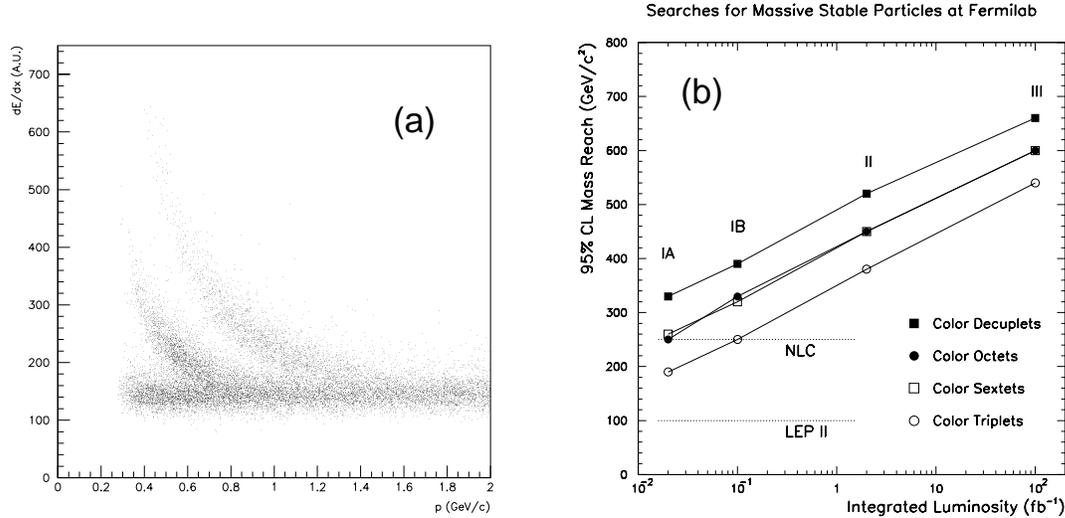


Figure 2.38: (a) A scatter plot of the  $\frac{dE}{dx}$  vs momentum is shown for the Run Ib silicon detector after a cut has been applied on the  $\frac{dE}{dx}$  from the main tracking chamber. Known particles (kaons and protons) can be clearly distinguished for  $p/m < 1.2$ , *i.e.*,  $\beta < 0.6$ . New massive particles would look similar but at higher momentum. (b) The expected mass reach is plotted vs. integrated luminosity at the Tevatron. The maximum mass reach of other accelerators is shown for comparison.

### 2.4.9 Technicolor

Technicolor assumes that pairs of fundamental techniquarks are bound into a composite scalar, a technipion, which generates a dynamical symmetry breaking. In recent technicolor models[37, 38] there exists a color octet technirho ( $\rho_T$ ) which couples to  $q\bar{q}$  and  $gg$  via a virtual intermediate gluon ( $\rho_T \rightarrow g \rightarrow q\bar{q}$ ,  $gg$ ) and would show up in the detector as dijets in all cases except when it decays into  $t\bar{t}$ . In the limit that the  $\rho_T$  branching ratio to dijets is 100% our present searches exclude the region  $250 \text{ GeV}/c^2 < M_{\rho_T} < 500 \text{ GeV}/c^2$ . We expect to have sensitivity to the mass region  $200 < M_{\rho_T} < 770$  with  $2 \text{ fb}^{-1}$ . A color singlet technirho, on the other hand, can couple to the  $W, Z$  and technipions ( $\Pi_T$ )[39]. It is currently thought that  $\Pi_T$  decays via  $\Pi_T^0 \rightarrow b\bar{b}$  and  $\Pi_T \rightarrow b\bar{c}$ , both of which would show up as (tagged) dijets. The branching ratios into the various decay modes depend heavily on the masses of the  $\rho_T$  and  $\Pi_T$ . In many of the other cases ( $WW, WZ, W\Pi$ ) cases there is also a  $W+2$  Jet signal, for which searches are underway.

### 2.4.10 Charged Higgs Search

An expanded Higgs sector containing charged Higgs bosons is a persistent feature of candidate theories

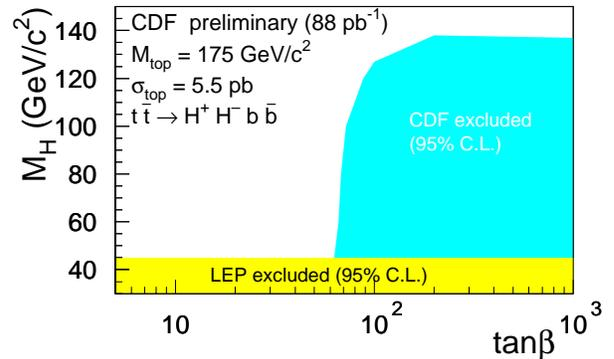


Figure 2.39: The charged Higgs exclusion region in charged Higgs mass vs.  $\tan\beta$  plane.

to replace the Standard Model. The minimal supersymmetric extension of the Standard Model, for example, predicts that the dominant decay mode of the top quark is  $t \rightarrow H^+ b \rightarrow \tau^+ \nu b$  for large values of  $\tan\beta$ . CDF has excluded charged Higgs production with  $M_{H^\pm} < 140 \text{ GeV}/c^2$  for large values of  $\tan\beta$  using the hadronic decays of the tau lepton in this channel using Run Ib data.(see Fig 2.39). Currently, background from jets which mimic a tau lepton limit this analysis. However, the larger data samples of

Searches for New Physics at Fermilab ( $\sqrt{s}=2$  TeV)

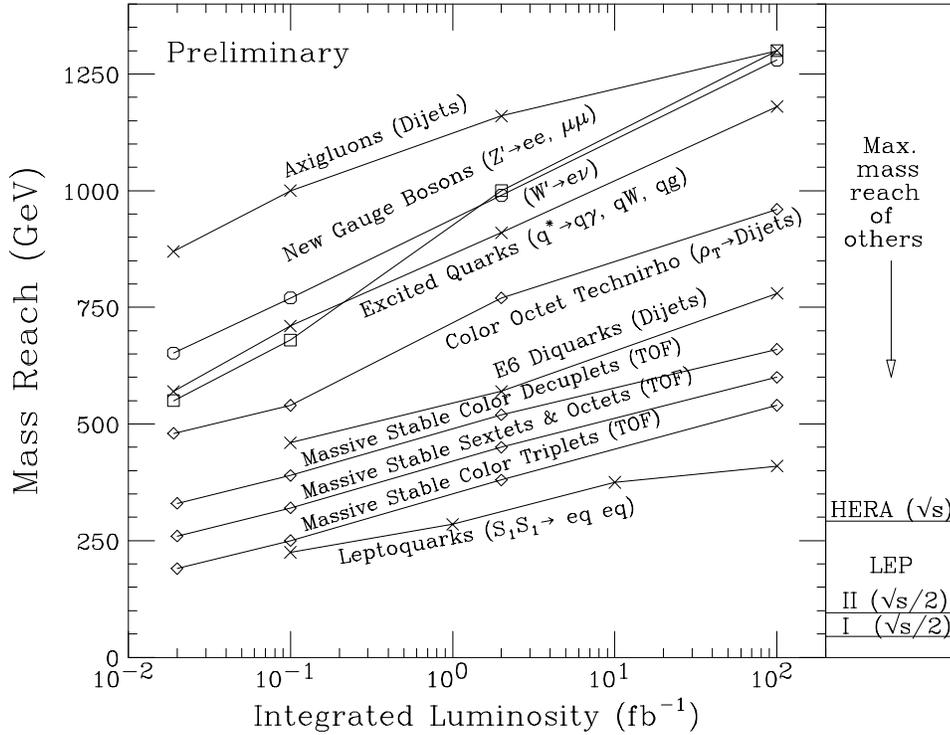


Figure 2.40: The mass reach of CDF II, defined as the 95% C.L. lower limit on the mass, is plotted for several new physics models as a function of integrated luminosity at the Tevatron. The maximum mass reach of other accelerators is shown for selected processes.

Run II will allow better determination of all of the backgrounds and will offer the opportunity to look for charged Higgs pair production to extend the limit to lower  $\tan\beta$ .

### 2.4.11 Summary

CDF has produced most of the current highest limits in direct searches for physics beyond the Standard Model. This experience allows us to make realistic predictions of how the additional luminosity obtained in Run II will substantially extend our reach for new physics, as summarized in Figure 2.40 and Table 2.10. The prospects of exploring the regions opened to us in Run II with integrated tracking with better pattern recognition, improved calorimeter, tracking, muon, and  $b$ -tagging coverage, and the ability to trigger on  $b$  jets are immensely exciting.

# Bibliography

- [1] G.W. Anderson and D.J. Castaño, hep-ph/9509212, Phys. Rev. **D53**, 2403 (1996).
- [2] S. Dimopoulos, M. Dine, S. Raby, and S. Thomas, hep-ph/9601367, Phys. Rev. Lett. **76**, 3494 (1996); S. Dimopoulos, S. Thomas, J.D. Wells, hep-ph/9604452 and preprint SLAC-PUB-7148 (1996).
- [3] S. Ambrosanio, G. Kane, G. Kribs, S. Martin, and S. Mrenna, hep-ph/9602239, Phys. Rev. Lett. **76**, 3498 (1996).
- [4] S. Ambrosanio, G. Kane, G. Kribs, S. Martin, and S. Mrenna, hep-ph/9605398 (1996).
- [5] K.S. Babu, C. Kolda, and F. Wilczek, hep-ph/9605408 (1996).
- [6] J.L. Lopez and D.V. Nanopoulos, hep-ph/9607220 and preprint CTP-TAMU-23/96 (1996).
- [7] K. Lane, and E. Eichten, BUHEP-95-11, Mar 1995; hep-ph/9503433; Phys. Lett. **B352**, 382, (1995).
- [8] V. Barger, K. Cheung, and P. Langacker, preprint MADPH-96-936, April 1996.
- [9] C. Hill and S. Parke, Phys. Rev. **D49**, 4454 (1994).
- [10] C. Hill and X. Zang, Fermilab-PUB-94/231-T (1994).
- [11] C. Hill, Phys. Lett. **B345**, 483 (1995); hep-ph/9411426
- [12] In all of the new particle searches discussed here, except for the dijet and b-tagged dijet searches, there are almost no events in the mass region where the limits are set. To obtain a number for the Run II extrapolation, we assume this will remain the case so that the cross section limit will roughly scale inversely with luminosity. In the dijet and b tagged dijet mass searches, there are significant backgrounds in the search region so the cross section limit will scale inversely with the square root of the luminosity.
- [13] The TeV-2000 Group Report, Fermilab-PUB-96/082. See Section 6 (Supersymmetric Physics) and Section 7 (Prospects for Exotic Physics at the Tevatron).
- [14] D.V. Volkov and V.P. Akulov, Phys. Lett. **46B**, 109 (1973); J. Wess and B. Zumino, Nucl. Phys. **B70**, 39 (1974).
- [15] For reviews, see H.P. Nilles, Phys. Rep. **110**, 1 (1984); H.E. Haber and G.L. Kane, Phys. Rep. **117**, 75 (1985).
- [16] For a recent review, see J.L. Lopez, "Supersymmetry: From the Fermi Scale to the Planck Scale," hep-ph/9601208, to appear in Report on Progress in Physics.
- [17] M. Dine, W. Fischler, and M Srdnicki, Nucl. Phys. **B189**, 575 (1981); S. Dimopoulos and S. Raby, Nucl. Phys. B192, **353** (1981). For a more recent view, see M. Dine, A.E. Nelson, and Y. Shirman, Phys. Rev. **D51**, 1362, (1995).
- [18] P. Nath and R. Arnowitt, Mod. Phys. Lett. **A2**, 331 (1987); R. Barbieri, F. Caravaglios, M. Frigeni and M. Mangano, Nucl. Phys. **B367**, 28 (1991); H. Baer and X. Tata, Phys. Rev. **D47**, 2739 (1993); J.L. Lopez, D.V. Nanopoulos, X. Wang and A. Zichichi, Phys. Rev. **D48**, 2062 (1993); H. Baer, C. Kao, and X. Tata, Phys. Rev. **D48**, 5175 (1993).
- [19] H. Baer, X. Tata, and J. Woodside, Phys. Rev. **D45**, 142 (1992).
- [20] F. Abe *et al.* (CDF Collaboration), Phys. Rev. Lett. **76**, 4307 (1996).

- [21] For a recent review, see R. Arnowitt and P. Nath, "Supersymmetry and Supergravity: Phenomenology and Grand Unification," Proceedings of VII<sup>th</sup> J.A. Swieca Summer School, Campos de Jordao, Brazil, 1993 (World Scientific, Singapore, 1994).
- [22] L.E. Ibañez, C. Lopez, and C. Muñoz, Nucl. Phys. **B256**, 218 (1985). G.G. Ross and R.G. Roberts, Nucl. Phys. **B377**, 571 (1992); R. Arnowitt and P. Nath, Phys. Rev. Lett. **69**, 725 (1992); S. Kelley, J.L. Lopez, D.V. Nanopoulos, H. Pois, and K. Yuan, Nucl. Phys. **B398**, 31 (1993); G.L. Kane, C. Kolda, L. Roszkowski, and J.D. Wells, Phys. Rev. **D49**, 6173 (1994). We used an approximate formula ( $\tilde{l}$  and  $\tilde{\nu}$  masses to  $\tilde{q}$  and  $\tilde{g}$  masses) in H. Baer *et al.*, Phys. Rev. **D47**, 2739 (1993).
- [23] ALEPH Collaboration, CERN-PPE/96-10, submitted to Phys. Lett. B (1996); OPAL Collaboration, CERN-PPE/96-20, submitted to Phys. Lett. B (1996).
- [24] J.L. Lopez, D.V. Nanopoulos, and A. Zichichi, Phys. Rev. **D52**, 4178 (1995). Input parameters for ISAJET are provided by J.L. Lopez.
- [25] T. Kamon, J.L. Lopez, P. McIntyre, and J.T. White, Phys. Rev. D **50**, 5676 (1994).
- [26] S. Mrenna, G.L. Kane, G.D. Kribs, and J.D. Wells, "Possible Signals of Constrained Minimal Supersymmetry at a High Luminosity Fermilab Tevatron Collider," hep-ph/9505245, CIT 68-1986, UM-TH-95-14 (1995).
- [27] H. Baer, C.-H. Chen, C. Kao, and X. Tata, "Supersymmetry Reach of an Upgraded Tevatron Collider," hep-ph/9504234, FSU-HEP-950301, UR-1411, UH-511-826-95 (1995).
- [28] H. Baer *et al.*, Phys. Rev. **D36**, 96 (1987).
- [29] F. Abe *et al.* (CDF Collaboration), Phys. Rev. Lett. **76**, 2006 (1996).
- [30] See F. del Aguila, M. Quiros, and F. Zwirner, Nucl. Phys. **B287**, 457 (1987) and references therein.
- [31] For a review and original references see R. N. Mohapatra, "Unification and Supersymmetry," (Springer, New York, 1986).
- [32] F. Abe *et al.* (CDF Collaboration), Phys. Rev. Lett. **67**, 2609 (1991).
- [33] F. Abe *et al.* (CDF Collaboration), Fermilab-PUB-94/268-E, submitted to Phys. Rev. Lett.
- [34] G. Altarelli, B. Mele and M. Ruiz-Altaba, Z. Phys. **C45**, 109 (1989).
- [35] P. Frampton and S. Glashow, Phys. Lett. **B190**, 157 (1987).
- [36] C. Albajar *et al.* (UA1 Collaboration), Phys. Lett. **B209**, 127 (1988).
- [37] K. Lane and M. V. Ramana, Phys. Rev. **D44**, 2678 (1991).
- [38] E. Eichten and K. Lane, Phys. Lett. **B327**, 129 (1994).
- [39] K. Lane and E. Eichten, Phys. Lett. **B222**, 274 (1989).
- [40] J. Hewett and T. Rizzo, Phys. Rep. **C183**, 193 (1989).
- [41] F. Abe *et al.* (CDF Collaboration), Phys. Rev. Lett. **74**, 3538 (1995).
- [42] J. Pati and A. Salam, Phys. Rev. **D10**, 275 (1974).
- [43] J. Hewett and S. Pakvasa, Phys. Rev. **D37**, 3165 (1988).
- [44] W. Buckmüller and D. Wyler, Phys. Lett. **B177**, 377 (1986).
- [45] G. Valencia and S. Willenbrock, Phys. Rev. **D50**, 6843 (1994).
- [46] E. Eichten, K. Lane, and M. Peskin, Phys. Rev. Lett. **50**, 811 (1983).
- [47] U. Baur, I. Hinchliffe, and D. Zeppenfeld, Int. J. Mod. Phys. **A2**, 1285 (1987); U. Baur, M. Spira and P. Zerwas, Phys. Rev. **D37**, 1188 (1988).
- [48] F. Abe *et al.* (CDF Collaboration), FERMILAB-PUB-96/020-E; Submitted to Phys. Rev. Lett. January 1996.
- [49] J. Huston *et al.*, MSU-HEP-50812, FSU-HEP-951031, CTEQ-512 (1995).

- [50] E.W.N. Glover, A.D. Martin, R.G. Roberts, K.J. Stevenson and W.J. Stirling, DTP-96-22 (1996).
- [51] H.L. Lai, W.K. Tung, hep-ph/9605269 (1996).
- [52] F. Abe *et al.* (CDF Collaboration), Phys. Rev. Lett. **67**, 2418 (1991).
- [53] F. Abe *et al.* (CDF Collaboration), Phys. Rev. Lett. **68**, 1463 (1992).
- [54] J. Alitti *et al.* (UA2 Collaboration), Nucl. Phys. **B400**, 3 (1993).
- [55] F. Abe *et al.* (CDF Collaboration), Phys. Rev. Lett. **72**, 3004 (1994).
- [56] F. Abe *et al.* (CDF Collaboration), Phys. Rev. Lett. **63**, 1447 (1989).
- [57] F. Abe *et al.* (CDF Collaboration), Phys. Rev. **D46**, 1889 (1992).